Supplementary Information

Solid-phase synthesis of ultra-small CuMo solid solution alloy for efficient electroreduction CO_2-to-C_{2+}

Zhili Zhang [a], Jingwen Hu[a], Xuan Zheng[a], Wenchao Zhang[b], Shuanglong Lu[a], Fang Duan[a], Han Zhu[a*], Mingliang Du[a]*

[a]Key Laboratory of Synthetic and Biological Colloids, Ministry of Education, School of Chemical and Material Engineering, Jiangnan University, Wuxi, jiangsu 214122, P. R. China.
E-mail: zhysw@jiangnan.edu.cn
[b]School of Chemistry and Life Sciences, Suzhou University of Science and Technology, Suzhou, 215009, Jiangsu, P. R. China

Experimental

Materials

Copric chloride dihydrate ($CuCl_2{\cdot}2H_2O$, 99.9%) and ammonium molybdate tetrahydrate ($(NH_4)_6Mo_7O_{24}{\cdot}4H_2O$) were purchased from Shanghai Aldrich Biochemical Co., Ltd. Polyvinylpyrrolidone (PVP, M_w = 1 300 000), potassium hydroxide (KOH, 95%), deuterium oxide (D_2O, 99.9%) and dimethyl sulfoxide (C_2H_6SO, 99.7%) were obtained from Shanghai Macklin Biochemical Co., Ltd. N, N'-dimethylformamide (DMF, 99%), acetone (C_3H_6O, 99.7%) and ethanol anhydrous (C_2H_6O, 99.7%) were purchased from Sinopharm Chemical Reagent Co., Ltd. Carbon dioxide (CO_2, 99.9995%) and argon (Ar, 99.999%) were ordered from Xinxiyi Technology Co., Ltd. (Wuxi, China). Ultrapure water (Milli-Q) was used to prepare the aqueous solution. All the reagents were used without any further purification.

Synthesis of the CuMo salts/PVP nanofiber membrane

Electrospinning technology was used to prepare the precursors of solid solutions. In a typical procedure, $CuCl_2{\cdot}2H_2O$ and $(NH_4)_6Mo_7O_{24}{\cdot}4H_2O$ were added into 16 g DMF solution (the total mass of metal salt was 0.2 g). Then 2 g PVP powder was dissolved in the above solution after one hour and then vigorously stirred for 12 h at room temperature to get a homogeneous solution. After that, the mixed solution was transferred to 10 mL injection syringes with a needle diameter of 0.7 mm. During the electrospinning process, the temperature and humidity of the electrospinning machine (YFSP-T, Tianjin Yunfan Technology Co., Ltd.) were controlled at 30 ^oC and 40%. Besides, the anode voltage and cathode voltage were 18 kV and 2 kV, the distance between needle and metal roller was 18 cm and the injection rate was 0.6 mL h^{-1}. After 15 h, the as-obtained Cu-Mo salts/PVP nanofiber membrane was placed in the oven at 80 ^oC overnight to remove the residual moisture.

Synthesis of the CuMo/CNFs

The Cu-Mo salts/PVP nanofiber membrane was heated to 200 ^oC with a heating rate of 2 ^oC min^{-1} and maintained for 3 h under air atmosphere using a home-built chemical vapor deposition (CVD) system. Then, after the pre-oxide process, the membrane was continuously heated to 1100 ^oC with 2 ^oC min^{-1} under Ar atmosphere. Subsequently, the membrane was naturally cooling to room temperature and the CuMo solid solution alloy nanoclusters supported on carbon nanofibers (CuMo/CNFs) were obtained. Besides, a series of CuMo/CNFs with different mass loading of Cu and Mo metal salts (the total metal salt was 0.2 g, and the weight ratio of Cu and Mo metal salts were 3:1, 2:1, 1:1 and 1:2, named as Cu_3Mo_1/CNFs, Cu_2Mo_1/CNFs, Cu_1Mo_1/CNFs and Cu_1Mo_2/CNFs) were synthesized. As control, the individual Cu/CNFs and Mo_2C /CNFs without Mo or Cu element were also synthesized.

Materials characterizations

The morphologies of the as-prepared samples were collected by the field-emission scanning electron microscope (FE-SEM Hitachi S-4800, Japan) with an acceleration voltage of 3 kV and the transmission electron microscope (TEM, JEM-2100 plus, Japan) operated at 200 kV. The STEM images, mapping and energy dispersive X-ray spectrum (EDX) were aquired with a scanning transmission electron microscope (STEM, JEOL JEM-F200, Japan), using an acceleration voltage of 200 kV. The phase and structure of the samples were conducted on a Bruker AXS D8 X-ray diffraction (XRD) using Cu-K_α (λ=0.154 nm) with the scan rate of 5^o min^{-1}. X-ray photoelectron spectroscopy (XPS) measurements were analyzed by Thermo Scientific K-Alpha with a monochromatic Al K_α source (1486.6 eV). The content of the Cu and Mo in Cu_2Mo_1/CNFs was obtained by a inductively coupled plasma optical emission

spectroscopy (ICP-OES, Ahilent 5110). Raman measurements were conducted on the confocal Raman microscope with a 532 nm laser. The *in situ* Raman measurements were carried out using a Renishaw inVia confocal microscope at the excitation laser wavelength of 785 nm. Prepared catalysts served as the working electrode, Ag/AgCl and Pt wire worked as the reference electrode and counter electrode. The flowing KOH solution (1 M) with continuous CO_2 injection acted as the electrolyte. The *in situ* Raman spectra were collected using chronoamperometry tests from -0.1 to -1.2 V (vs. RHE) and each potential maintained at least 10 minutes for sufficient reaction.

Electrochemical measurements

The CO_2 reduction reaction (CRR) were performed using an Autolab 302N electrochemical workstation with a standard three-electrode system conducted on a commercial flow cell (Gaossunion) in 1 M KOH solution at room temperature. To prepare the ink of working electrode, 3 mg catalyst and 15 μL Nafion (5 wt%) were dispersed in the 300 μL ethanol solution and ultrasonicated for 30 min to obtain a homogeneous dispersion of catalyst ink. Then, the ink was airbrushed onto a carbon paper (Sigracet 29 BC) as working electrode (2 x 0.5 cm) and the loading mass is 0.5 mg cm^{-2}. The Ag/AgCl (3.0 M KCl) and Pt foil worked as the reference electrode and counter electrode, respectively. An anion exchange membrane (PAA-3-PK-130) was used to separate the anolyte and catholyte. The volumes of electrolyte in anode and cathode compartment were both 50 mL. In addition, The electrolyte (1 M KOH) was circulated through the flow cell by a bump with flowing rate of 10 mL min^{-1} during the CRR process. Besides, the CO_2 gas was controlled at 20 mL min^{-1} using the flowmeter. To analyze the gas-phase products of working electrode, the cathodic compartment was directly connected to the gas chromatograph (GC, Agilent 7890B) equipped with TCD and FID detectors. The liquid products were quantitatively analyzed by ^1H NMR on a Bruker 400 MHz (AVANCE Ⅲ) spectrometer with D_2O and DMSO acted as solvent and internal standard. The Faradaic efficiency (FE) of products were calculated by the equation: $FE=eF\times n/Q$, where e is the number of transfer electrons, F is the Faraday constant (96485 C mol^{-1}), n is the moles of the products, and Q is the total charge in the CRR process. The linear sweep voltammetry (LSV) was perfomered with sweep rate of 5 mV s^{-1}. The electrochemical impedance spectroscopy (EIS) was conducted at the open circuit voltage in the range from 10^{-2} Hz to 10^5 Hz. All potentials were converted to the reversible hydrogen electrode (RHE) according to Nernst equation :$E_{(vs.RHE)} = E_{(vs.\ Ag/AgCl)} + E_{Ag/AgCl} + 0.0591 \times pH$.

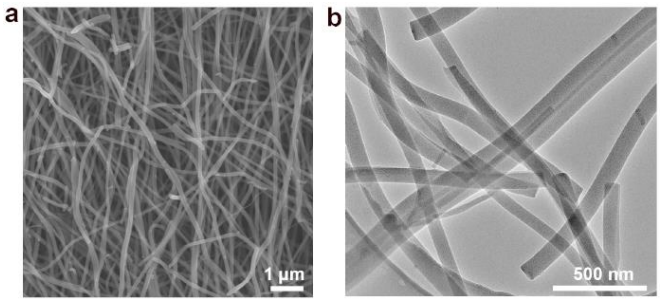

Fig. S1. Low-magnification of (a) SEM and (b) TEM images for Cu_2Mo_1/CNFs.

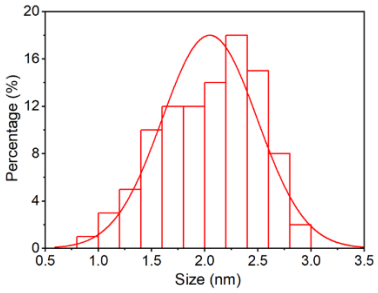

Fig. S2. Corresponding size distribution of Cu-Mo solid solution alloy nanoparticles in Cu_2Mo_1/CNFs.

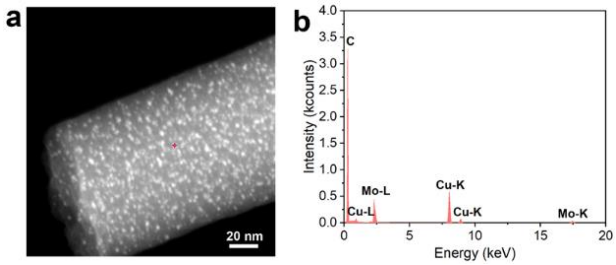

Fig. S3. STEM image and corresponding spot-scan EDX spectra of Cu_2Mo_1/CNFs.

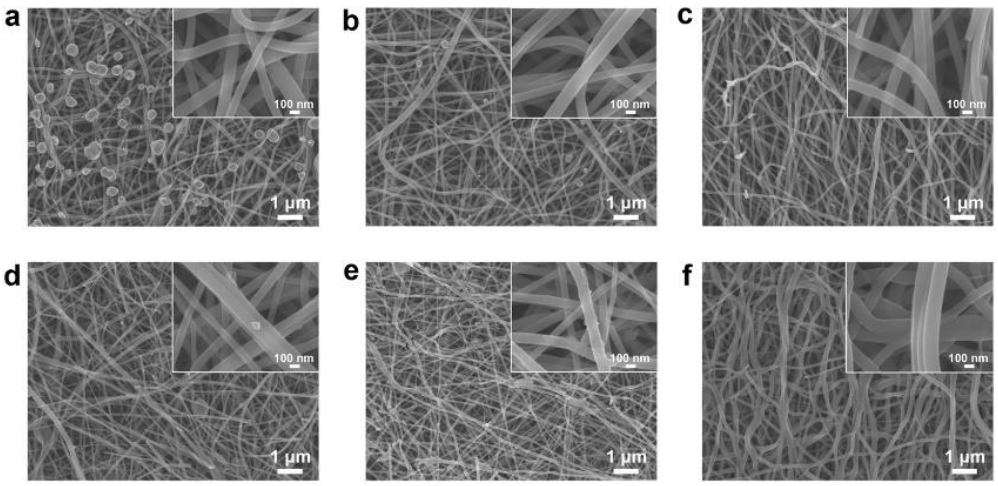

Fig. S4. SEM images of (a) Cu/CNFs, (b) Cu_3Mo_1/CNFs, (c) Cu_2Mo_1/CNFs, (d) Cu_1Mo_1/CNFs, (e) Cu_1Mo_2/CNFs and (f) Mo_2C/CNFs. Inset in (a-f) are the corresponding high-magnification SEM images.

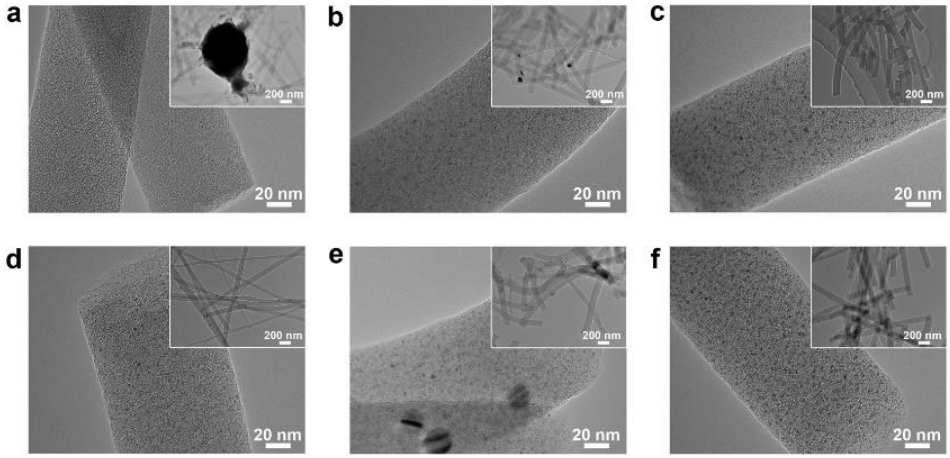

Fig. S5. TEM images of (a) Cu/CNFs, (b) Cu_3Mo_1/CNFs, (c) Cu_2Mo_1/CNFs, (d) Cu_1Mo_1/CNFs, (e) Cu_1Mo_2/CNFs and (f) Mo_2C /CNFs. Inset in (a-f) are the corresponding low-magnification TEM images.

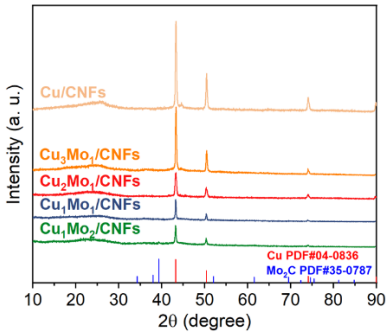

Fig. S6. XRD patterns of obtained samples.

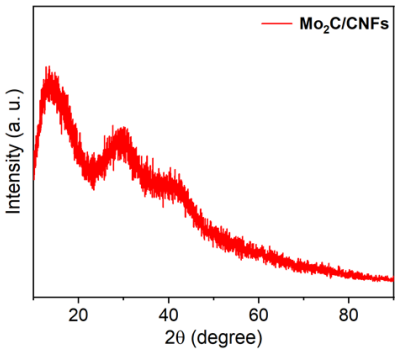

Fig. S7. XRD pattern of Mo_2C /CNFs.

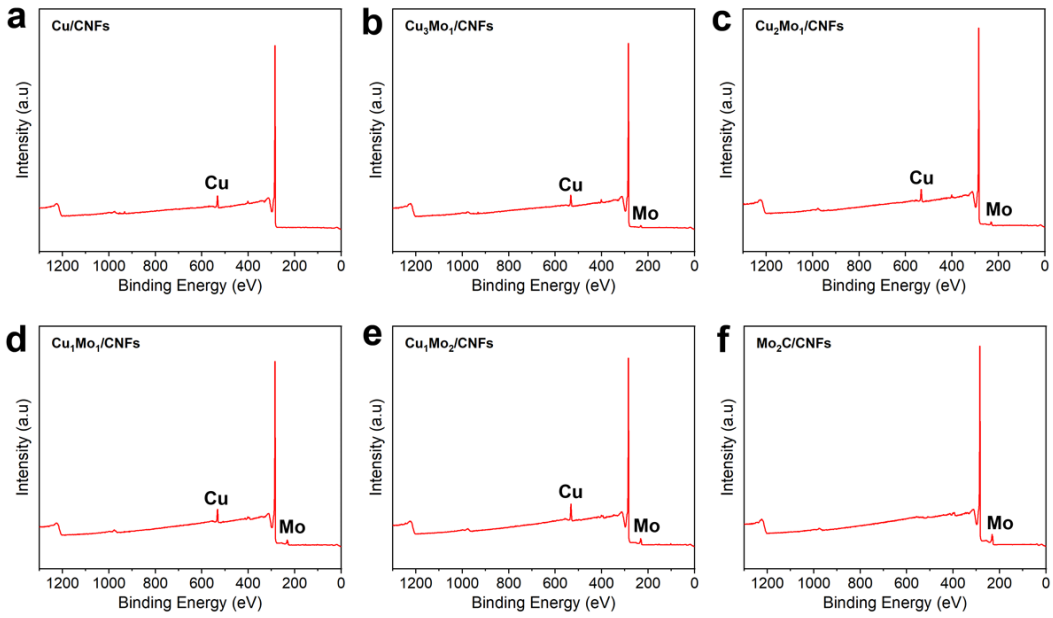

Fig. S8. XPS surveys of obtained samples.

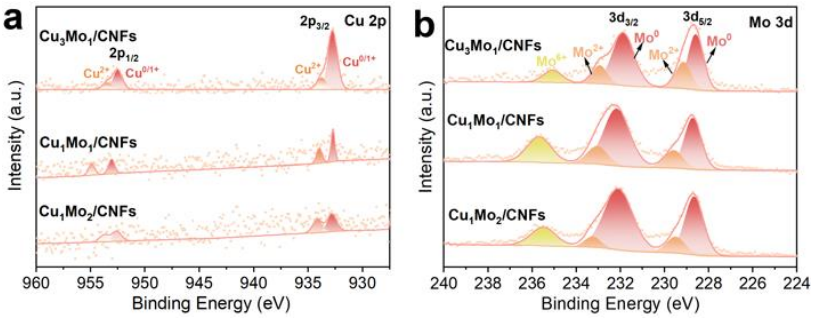

Fig. S9. XPS spectra of (a) Cu 2p and (b) Mo 3d for Cu_3Mo_1/CNFs, Cu_1Mo_1/CNFs and Cu_1Mo_2/CNFs.

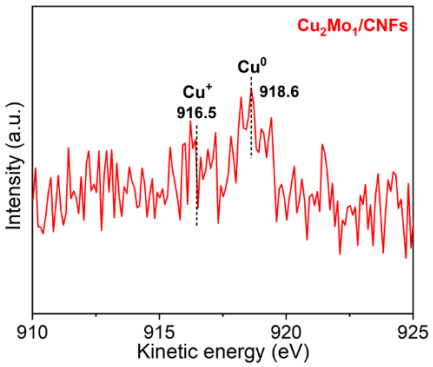

Fig. S10. The Cu LMM Auger spectrum of Cu_2Mo_1/CNFs.

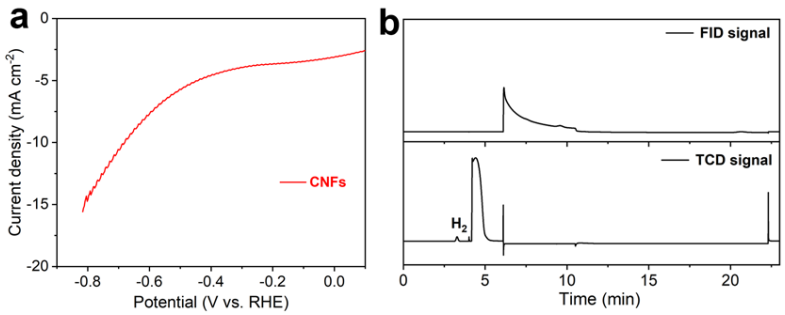

Fig. S11. LSV curve and GC signals of original carbon nanofibers.

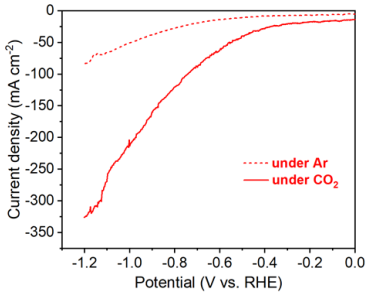

Fig. S12. LSV curves of Cu_2Mo_1/CNFs under CO_2 and Ar saturated 1 M KOH solution.

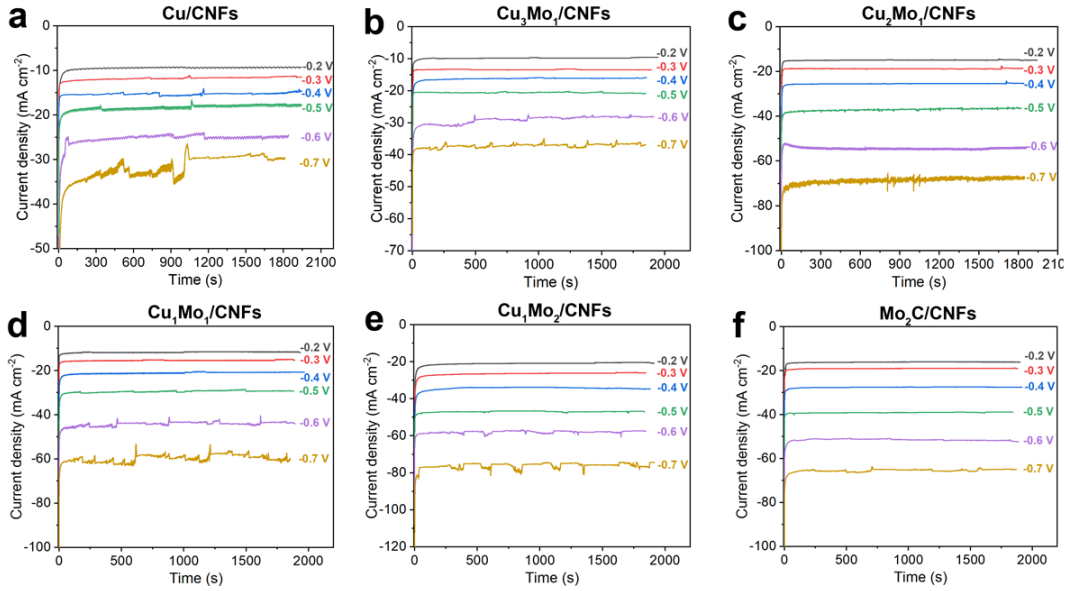

Fig. S13. I-t curves at various potentials of (a) Cu/CNFs, (b) Cu_3Mo_1/CNFs, (c) Cu_2Mo_1/CNFs, (d) Cu_1Mo_1/CNFs, (e) Cu_1Mo_2/CNFs and (f) Mo_2C /CNFs.

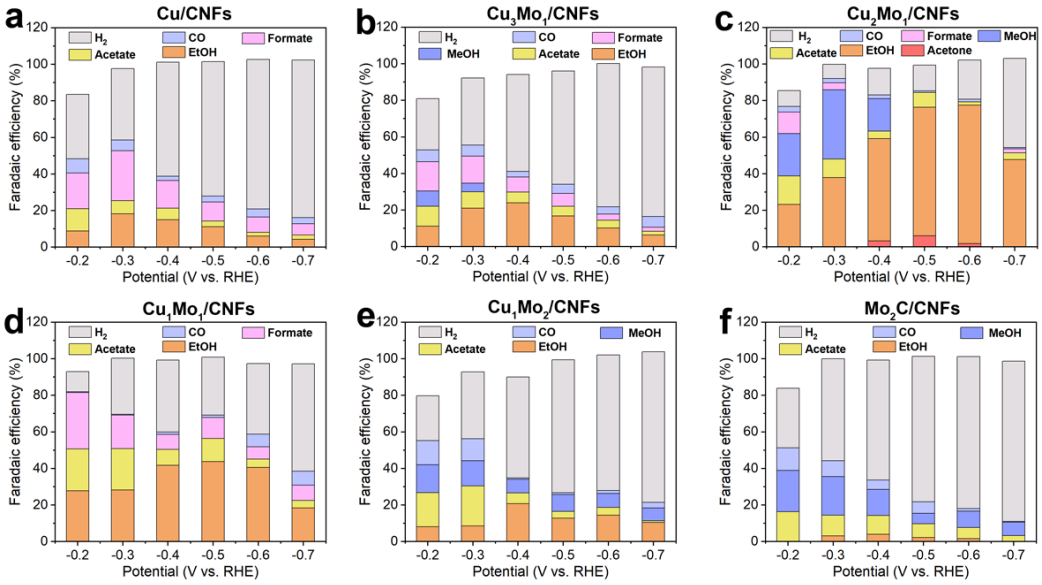

Fig. S14. Potential-dependent Faradaic efficiencies of products for (a) Cu/CNFs, (b) Cu_3Mo_1/CNFs, (c) Cu_2Mo_1/CNFs, (d) Cu_1Mo_1/CNFs, (e) Cu_1Mo_2/CNFs and (f) Mo_2C /CNFs.

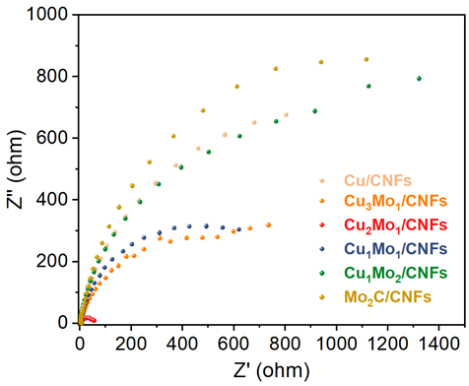

Fig. S15. EIS plots of obtained samples.

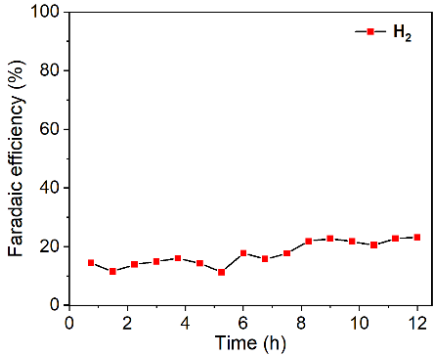

Fig. S16. FE of H_2 in stability test of Cu_2Mo_1/CNFs at the potential of -0.5 V.

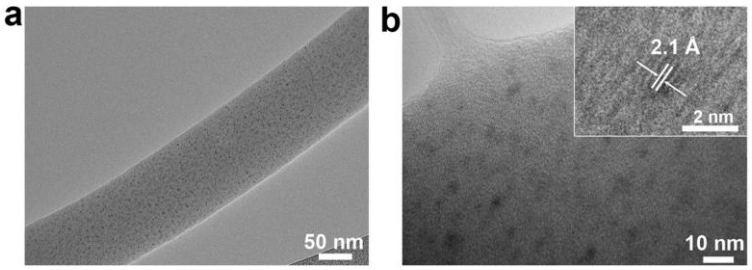

Fig. S17. (a) TEM and (b) HRTEM images of Cu_2Mo_1/CNFs after long-term stability test.

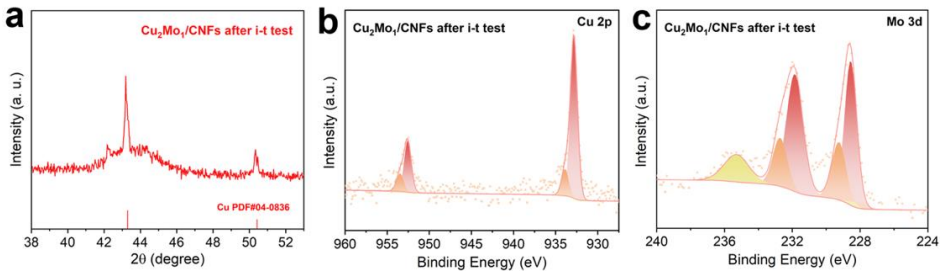

Fig. S18. (a) XRD pattern, (b) Cu 2p and (c) Mo 3d XPS spectra of Cu_2Mo_1/CNFs after long-term stability test.

Table S1. The loading amount of Cu and Mo in Cu_2Mo_1/CNFs determined by ICP-OES and EDS.

	Element	Content (wt%)
ICP-OES	Cu	22.80
	Mo	10.32
EDS	Cu	25.29
	Mo	11.09

Table S2. Detailed FEs of serious products in CO_2RR using Cu/CNFs as the catalyst.

E (v vs. RHE)	Ethanol (%)	Acetate (%)	Formate (%)	CO (%)	H_2 (%)	C_{2+} (%)	Total (%)
-0.2	8.8	12.3	19.5	7.8	35.1	21.1	83.5
-0.3	18.3	7.2	27.2	5.9	38.9	25.5	97.6
-0.4	15.0	6.3	15.1	2.3	62.4	21.4	101.2
-0.5	11.2	3.1	10.4	3.3	73.5	14. 3	101.5
-0.6	6.1	2.1	8.3	4.4	81.8	8. 2	102.6
-0.7	4.3	2.4	6.2	3.3	86.2	6.7	102.4

Table S3. Detailed FEs of serious products in CO_2RR using Cu_3Mo_1/CNFs as the catalyst.

E (v vs. RHE)	Ethanol (%)	Acetate (%)	Methanol (%)	Formate (%)	CO (%)	H_2 (%)	C_{2+} (%)	Total (%)
-0.2	11.2	10.9	8.3	16.1	6.4	28.1	22.1	80.9
-0.3	21.1	8.8	4.8	14.8	6.0	36.7	29.9	92.3
-0.4	24.0	5.9		8.2	3.1	53.0	29.8	94.1
-0.5	16.8	5.3		6.9	5.0	62.0	22.1	96.0
-0.6	10.2	4.3		3.3	4.0	78.4	14.5	100.2
-0.7	6.3	2.2		2.2	5.8	81.7	8.5	98.3

Table S4. Detailed FEs of serious products in CO_2RR using Cu_2Mo_1/CNFs as the catalyst.

E (v vs. RHE)	Acetone (%)	Ethanol (%)	Acetate (%)	Methanol (%)	Formate (%)	CO (%)	H_2 (%)	C_{2+} (%)	Total (%)
-0.2	0	23.3	15.5	23.3	11.6	3.2	8.5	38.8	85.4
-0.3	0	37.9	10.1	37.9	3.8	2.3	7.8	48.0	99.8
-0.4	3.3	55.9	4.1	17.8	0	2.0	14.6	63.3	97.7
-0.5	**6.1**	**70.2**	**8.2**	**0**	**0**	**0.9**	**14.0**	**84.5**	99.4
-0.6	**1.8**	**75.7**	**1.9**	**0**	**0**	**1.4**	**21.4**	**79.4**	102.2
-0.7	0	47.7	3.7	0	2.1	0.7	48.9	51.5	103.2

Table S5. Detailed FEs of serious products in CO_2RR using Cu_1Mo_1/CNFs as the catalyst.

E (v vs. RHE)	Ethanol (%)	Acetate (%)	Formate (%)	CO (%)	H_2 (%)	C_{2+} (%)	Total (%)
-0.2	27.8	22.9	30.9	0.3	11.0	50.7	92.9
-0.3	28.3	22.6	18.2	0.5	30.6	50.9	100.3
-0.4	41.7	8.7	8.1	1.4	39.3	50.4	99.2
-0.5	43.8	12.6	11.4	1.3	31.7	56.4	100.8
-0.6	40.6	4.5	6.8	6.8	38.6	45.1	97.3
-0.7	18.4	4.0	8.4	7.6	58.7	22.5	97.2

Table S6. Detailed FEs of serious products in CO_2RR using Cu_1Mo_2/CNFs as the catalyst.

E (v vs. RHE)	Ethanol (%)	Acetate (%)	Methanol (%)	CO (%)	H_2 (%)	C_{2+} (%)	Total (%)
-0.2	8.1	18.6	15.3	13.3	24.4	26.7	79.7
-0.3	8.6	21.7	13.9	12.0	36.6	30.4	92.8
-0.4	20.7	5.9	7.4	0.8	55.2	26.7	90.1
-0.5	12.9	3.7	9.2	1.1	72.5	16.5	99.4
-0.6	14.4	4.3	7.6	1.6	74.1	18.8	102.0
-0.7	10.4	0.9	7.2	3.0	82.3	11.3	103.8

Table S7. Detailed FEs of serious products in CO_2RR using Mo_2C /CNFs as the catalyst.

E (v vs. RHE)	Ethanol (%)	Acetate (%)	Methanol (%)	CO (%)	H_2 (%)	C_{2+} (%)	Total (%)
-0.2		16.3	22.7	12.2	32.6	16.3	83.8
-0.3	3.2	11.2	21.1	8.7	55.7	14.4	100.0
-0.4	4.1	10.3	14.1	5.2	65.6	14.4	99.3
-0.5	2.3	7.5	5.6	6.3	79.5	9.8	101.2
-0.6	1.6	6.2	8.9	1.4	83.1	7.8	101.2
-0.7		3.3	7.3	0.5	87.6	3.3	98.7